Original Article

A comprehensive investigation of computational fluid dynamics (CFD) wind flow simulation with a 3D building model

Nurfairunnajiha Ridzuan*, Uznir Ujang, and Suhaibah Azri

3D GIS Research Lab, Faculty of Built Environment and Surveying,
Universiti Teknologi Malaysia, Johor, 81310 Malaysia

Abstract

The buildings can influence wind flow, while a better wind flow in a city will improve the air quality for the sustainable development of the urbanites. At present, Computational Fluid Dynamics (CFD) is commonly used for wind flow simulation. However, CFD simulation is able to focus only on a certain height of a building. Hence, the 3D building model Level of Details (LoD) plays a vital role in the simulation. As regards the 3D building model standard, CityGML standard provides different LoD such as LoD1.0, LoD1.1, LoD1.2, LoD1.3, LoD2.0, LoD2.1, LoD2.2, LoD2.3, LoD3.0, LoD3.1, LoD3.2 and LoD3.3. Thus, this study aimed to overcome this problem by determining the best 3D building model's LOD for CFD wind movement simulation. This study ran CFD simulation experiments on each stated LoD using the same 3D model building. Several important points (locations) at the building were selected and analysed to obtain the best wind velocity analysis for the LoDs. Through such analysis, LoD3.1 was selected as the model that fulfils the minimum requirements to have the best CFD wind flow simulation. This research can help future planning of cities towards realizing sustainable city development by taking into account the factors affecting wind movement in the city.

Keywords: wind flow, wind velocity, CFD, CityGML, LoD

1. Introduction

The wind flow can be digitally visualized by using Computational Fluid Dynamics (CFD). Many related studies have been performed. However, researchers avoid performing simulations, especially over a city area that covers too large spatial extent, because this would increase the processing time and require very high computer hardware specifications (Piepereit Deininger, Kada, Pries, & Voß, 2018). Despite this problem, CFD simulation is compatible with Computer-Aided Design (CAD) standard only (Bettermann, Kandelhard, Moritz, & Pauer, 2019; Lee Park, Jang, & Kim, 2021; Triscone *et al.*, 2016).

In this study, the building model is included because the wind tends to flow or divert at a given angle in the simulation environment, depending on the building's geometric shape (Biao, Cunyan, Lu, Weihua & Jing, 2019). Nonetheless, this study proposes using the CityGML standard instead of CAD because it can assist in displaying the detailed geometry of building models by referring to an international standard for 3D building modelling (Kutzner, Chaturvedi, & Kolbe, 2020). There are five main levels of detail (LoD): LoD0, LoD1, LoD2, LoD3 and LoD4 (Biljecki, Stoter, Ledoux, Zlatanova & Çöltekin, 2015). Research by Deininger *et al.* (2020) emphasizes using a building model with LoD1 only, but, in this study, the more detailed LoDs are included. Differences in details between the LoDs are explained in Section 2.2.

There are many types of prior studies on 3D modelling of the different LoDs. For example, modelling indoor and outdoor building environments (Tang, Li, Ying, & Lei, 2018). Besides, modelling 3D cities and landscapes (Ohori, Biljecki, Kumar, Ledoux, & Stoter, 2018), multiscale analysis of cultural heritage (Colucci, Ruvo, De, Matrone, & Rizzo, 2020), flood modelling (Jang, Park, Kwon, & Lee, 2021), and noise mapping (Lu, Becker, & Lowner, 2017) are some of the applications that utilize this concept.

*Corresponding author
 Email address: nurfairunnajiha2@graduate.utm.my

As this study focuses on the exterior building geometry that can exist in an urban area, only LoD1, LoD2 and LoD3can be included. LoD0 cannot be used as it only represents the ground surface with no 3D building model and LoD4 adds on interior building information. Each LoD that is employed can be further broken into more detailed levels. LoD1 is divided into LoD1.0, LoD1.1, LoD1.2 and LoD1.3 (Biljecki, Ledoux & Stoter, 2016), and the same goes for LoD2 and LoD3. So, this research uses all these LoDs to see the effects of choice of LoD on the flow or movement of wind in an area when using CFD simulation.

2. Methodology

Figure 1 shows the methods involved in conducting this study. The whole process is divided into five phases: data acquisition, modelling, simulation, analysis and result validation. Each phase has a different specified purpose.

2.1. Data acquisition

No real-world building data is acquired, but only the 3D self-generated building model is used by following the level of detail standard introduced by CityGML. There are 12 different LoDs of building models to be generated: LoD1.0, LoD1.1, LoD1.2, LoD1.3, LoD2.0, LoD2.1, LoD2.2, LoD2.3, LoD3.0, LoD3.1, LoD3.2, and LoD3.3. Besides, wind data are needed for the CFD simulation to show the flow of wind surrounding the building model. Wind speed of 1.0 m/s (standard wind speed) is used because this research focuses only on showing the movement or flow of wind from a single direction, which is from the front side of a self-generated building, without the need to obtain real-world wind data.

2.2. Data modelling

In LoD1.x with further detail modelling can only be represented by a building block with no roof or other structures. Following that, in LoD2.x, all these models can be represented by adding a roof to models from LoD1.x; and the models from this LoD added with opening and any detailed exterior structures are to be presented in LoD3.x. The detailed standard to generate each model is shown in Figure 2. No interior structures or furniture are included as this study covers the exterior of a building.

2.3 Data simulation

The simulation used is CFD wind simulation in Rhino CFD software applying Chen-Kim k-ε turbulence model. Also, the governing equations are applied and computationally solved in the wind simulation environment. The equations formulated are based on the concept of conservation of physical properties: conservation of mass (Continuity Equation), conservation of momentum (Newton's Second Law), and conservation of energy (First Law of Thermodynamics) (Tey, Asako, Sidik, & Goh, 2017; Zawawi *et al.*, 2018). Stated below are the general equations for these three conservation laws, conservation of mass (Equation 1), conservation of momentum (Equation 2), and conservation of energy (Equation 3).
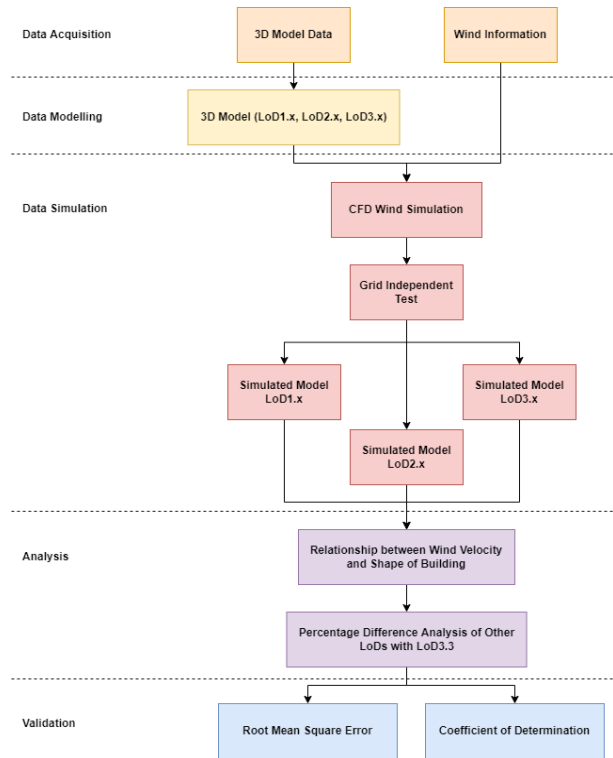

Figure 1. Flowchart of process wind flow simulation.

Requirements	Refined levels of detail															
	0.0	0.1	0.2	0.3	1.0	1.1	1.2	1.3	2.0	2.1	2.2	2.3	3.0	3.1	3.2	3.3
Individual buildings	•	•	•		•	•	•	•	•	•	•	•	•	•	•	•
Large building parts (>4 m, 10 m²)	•	•	•		•	•	•	•	•	•	•	•	•	•	•	•
Small building parts, recesses and extensions (>2 m, 2 m²)		•	•			•	•		•	•	•	•	•	•	•	•
Top surface[0]		S	M		S	S	S	M								
Explicit roof overhangs (if >0.2 m)											•		•	•	•	•
Roof superstructures[1] (larger than 2 m, 2 m²)										•	•	•	•	•	•	•
Other roof details (e.g. chimneys >1 m)												•		•	•	•
Openings[2] (>1 m, 1 m²)													R	W	•	•
Balconies (>1 m)													•	•	•	•
Embrasures, other façade and roof details, and smaller windows (>0.2 m)																•

[0] Applicable only to LOD0.y and LOD1.y: S—Single top surface; M—Multiple top surfaces if the difference in height of the extruded building elements is significant (larger than 2 m).
[1] It includes dormers and features of comparable size and importance (e.g. very large chimneys).
[2] R—only openings on roofs; W—only openings on walls. In R, openings on dormers are not required.

Figure 2. Characteristics of building models that need to be followed for different LoDs (Biljecki *et al.*, 2016).

$$\frac{D\rho}{Dt} + \rho \frac{\partial U_i}{\partial x_i} = 0 \tag{1}$$

$$\underbrace{\rho \frac{\partial U_j}{\partial t}}_{i} + \underbrace{\rho U_i \frac{\partial U_j}{\partial x_i}}_{ii} = \underbrace{-\frac{\partial P}{\partial x_j}}_{iii} - \underbrace{\frac{\partial \tau_{ij}}{\partial x_i}}_{iv} + \underbrace{\rho g_j}_{v} \tag{2}$$

$$\underbrace{\rho c_\mu \frac{\partial T}{\partial t}}_{I} + \underbrace{\rho c_\mu U_i \frac{\partial T}{\partial x_i}}_{II} = \underbrace{-P \frac{\partial U_i}{\partial x_i}}_{III} + \underbrace{\lambda \frac{\partial^2 T}{\partial x_i^2}}_{IV} - \underbrace{\tau_{ij} \frac{\partial U_j}{\partial x_i}}_{V} \qquad (3)$$

where I is local change with time, II is the convection term, III is surface force term, IV is molecular-dependent momentum exchange, and V is a mass force term.

In addition, for this CFD simulation, data of the building models, wind speed, and the inlet and outlet of wind flow in a domain are provided to help the simulation run smoothly. Besides, grid independence test is also performed to make sure the simulation presents accurate results with an optimum grid design (Lee, Park, Park, & Kim, 2020).

2.4 Analysis

In the first analysis, several parts of the building (Figure 3) that experience changes in shapes (referring to the most detailed model) along the simulation plane will be labelled alphabetically. At the same time, as the shape, for example, in LoD1.1 model only covers the outer part of the building, shapes that are too detailed as in LoD3.3 cannot be obtained in LoD1.1. Hence, this part will be not labelled in the LoD1.1 model. The same thing happens to other models that encounter the same problem. Next, some parts in LoD3.3 will not be labelled because there are no distinct changes in wind velocity compared to the neighbouring selected point. Thus, the relationship between changes in shapes of the building model and the wind velocity can be presented through the analysis process.
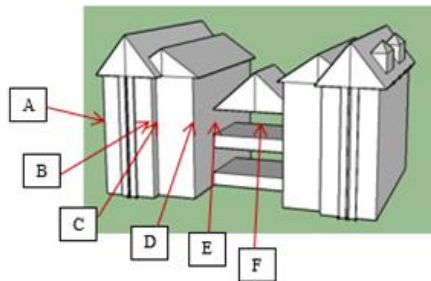

Figure 3. Selected points on building surface that are used in analysis phase.

For the wind velocity, from the simulation results, only the range of wind velocities at every point was recorded. However, an average from the selected range was used to produce a good and easy-to-interpret graph to assess wind velocity and shapes in each LoD.

The second analysis was carried out after acquiring the wind velocity values for each point on each LoD. This analysis entails determining the best model for simulated airflow that surrounds the building. To this purpos, the percentage difference at each point between wind velocity from LoD1.0 to 3.2 and wind velocity from LoD3.3 was determined, as the latter was used as a reference because of its detailed representation that portrays the real world, calculated by using Equation (4).

Difference (%) = |Reference − Observed|/ (4)
　　　　　　　　Reference × 100

Here Difference (%) represents the percentage difference between wind velocities, Reference means the velocity value for the point in LoD3.3, and Observed is the wind velocity for that point in the other LoDs.

2.5 Validation

To validate the percentage difference analysis results, the root mean square error (RMSE) was applied to the wind velocity data at all points of the 11 LoDs involved, compared with the all the wind velocity data for LoD3.3. Computation of the RMSE is done following Equation (5). Moreover, the coefficient of determination, R^2 is added to enhance the selection process of the optimum LoD, which involves the average velocity, v_a, and the heights respective to the domain, z_d.

$$RMSE = \sqrt{\frac{\sum(P_i - O_i)^2}{n}} \qquad (5)$$

where RMSE stands for root mean square error, P_i for predicted wind velocity value, O_i is the observed wind velocity value and n is the total number of points used to collect the wind velocity data.

3. Results and Discussion

3.1 3D Building model

There are 12 different generated 3D building models of various designs and levels of detail. So, it is easier to differentiate between buildings of different LoD (Figure 4).

	LoDx.0	LoDx.1	LoDx.2	LoDx.3
LoD1				
LoD2				
LoD3				

Figure 4. Building models used for CFD simulation.

3.2 CFD Simulation

Each CFD yielded a residual error below two percent, showing that the numerical simulation had converged (Concentration, Heat and Momentum [CHAM], 2020). Additionally, the grid independence test was run on each set of simulation results from different LoDs; Figure 5 illustrates the test results for one of the LoDs (LoD3.3). The results are documented in this section to help show an optimal grid for the CFD wind simulation. As referred in the figure, the marked fineness of grid was chosen as the practical optimum grid, since the variations after the marked point in results are not significant. Besides, the wind velocity selected for each of the simulations involved is along the Y-axis (U_y), as it can show significant differences to determine the optimum grid. In

this section, the simulation results are presented in a single figure that includes LoD1 models, LoD2 models, and LoD3 building models (Figure 6).
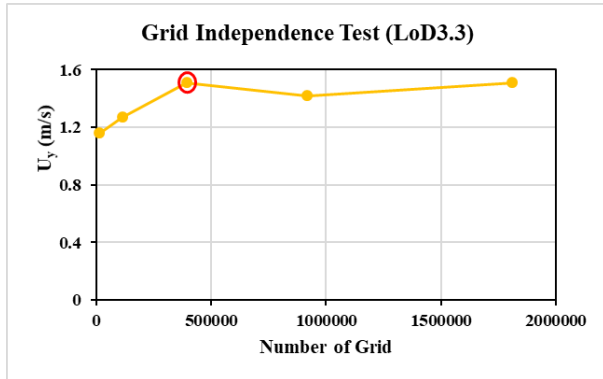
Grid Independence Test (LoD3.3)

Figure 5.   Grid independence test of LoD3.3

3.3 Data analysis and validation

The analysis results (Figure 7) show some differences in the average wind velocity portrayed by different LoDs resulting from different shapes represented by the points. First, for the LoD1.0 graph with a trend of only two points of available values, Point A has a higher wind velocity than Point B, at 1.951 m/s versus only 0.361 m/s for Point B. This is because the other points cannot be mapped on the model as it is just a building block compared to the other models that have more complex designs. Point A is a shape that exists at the edge of a building model.

Meanwhile, Point B is where a straight building wall exists. So, the velocity at the edge of the building is higher compared to the windward side (Liu, Niu, Mak & Xia, 2017; van Druenen, van Hooff, Montazeri & Blocken, 2019). Next is LoD1.1. Point A also shows the highest value (1.891 m/s) because this point represents the lateral side of the building model, which experiences no recirculation of wind flow that causes it to decrease in value; whereas the three points (B, E and F) have the lowest velocity – 0.196 m/s because of the downwash effect that leads to recirculation of flow (Chatzimichailidis, Argyropoulos, Assael, & Kakosimos, 2019; Liu *et al.*, 2017). Point C has no value because the point does not exist in the model, but, point D has a slightly higher value because this location has no direct effect from recirculation.

LoD1.2. The lowest value is portrayed by Point C (0.065 m/s), and the highest is at Point A (1.886 m/s). The fastest wind velocity obtained in the simulation for LoD1.3 is 1.792 m/s at points A and C, resulting in only 0.062 m/s. Besides, in the other graphs, point A also displayed the highest wind velocities of 1.715 m/s for LoD2.0, 1.747 m/s for LoD2.1, 1.744 m/s for LoD2.2, 1.754 m/s for LoD2.3, and 1.746 m/s for LoD3.0. Meanwhile, point C is that point which experiences the lowest wind speed in all remaining graphs, such as LoD2.0m/s), LoD2.1 (0.076 m/s), LoD2.2 (0.076m/s), LoD2.3 (0.076 m/s), and LoD3.0 (0.075 m/s). From the results, a third trend is portrayed in the graphs for LoD1.2 to LoD3.0. The generated wind velocities for points A, B, D, E and F are the same as earlier. However, there is one additional point with an available wind velocity, which is point C. The velocity at this point is the lowest compared to the others in this trend as the point is somehow in a closed area. Although
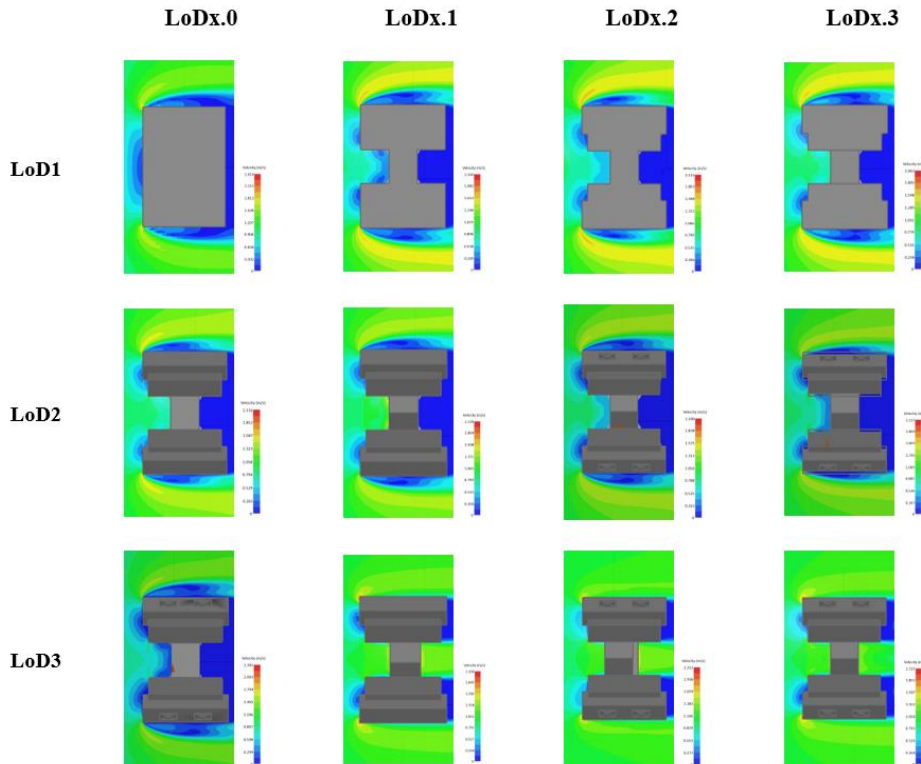

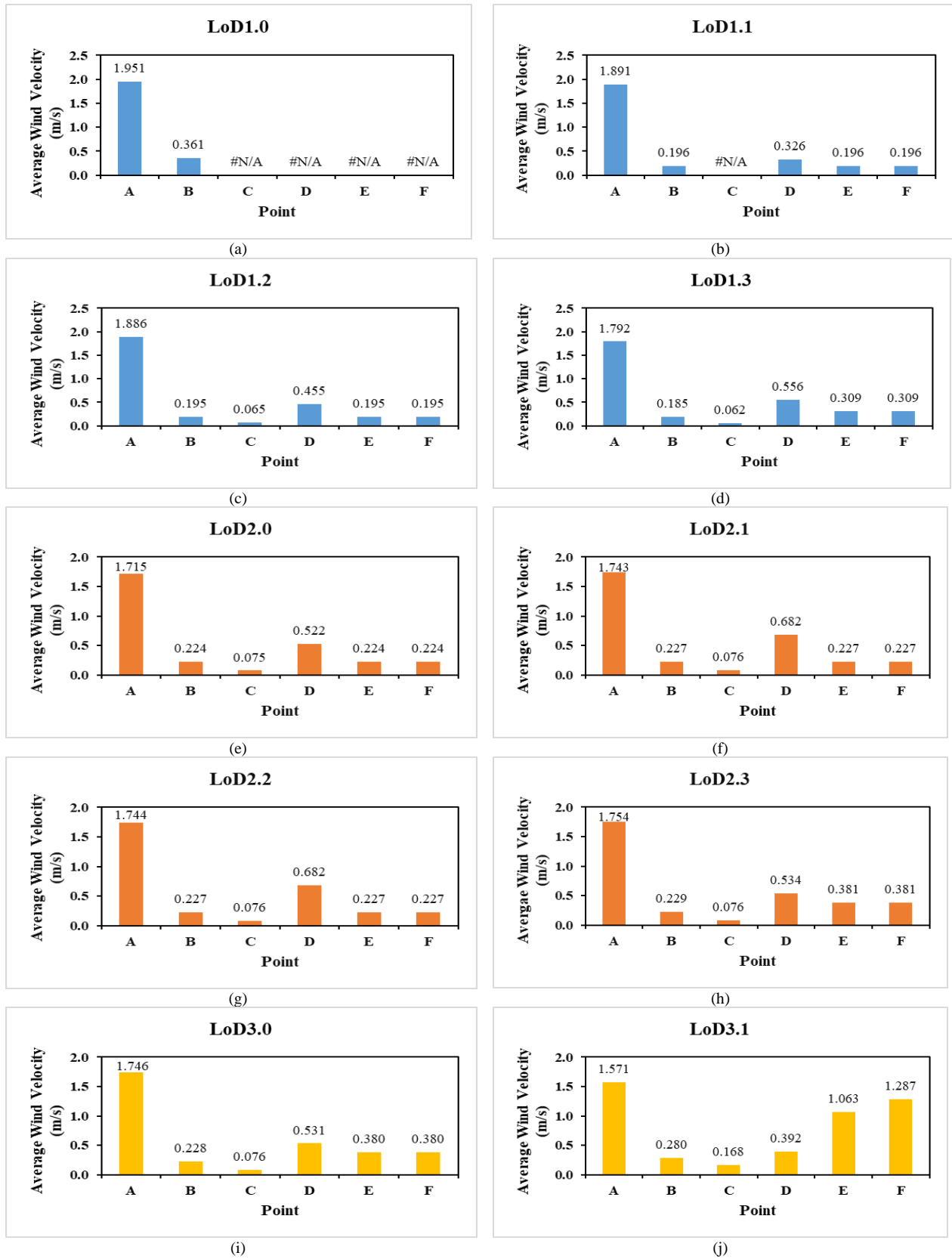Figure 6.   CFD simulation for all LoDs of building models

Figure 7.   Average wind velocity from CFD simulation for 12 different LoDs at labeled points selected for comparison. (a) LoD1.0, (b) LoD1.1, (c) LoD1.2, (d) LoD1.3, (e) LoD2.0, (f) LoD2.1, (g) LoD2.2, (h) LoD2.3, (i) LoD3.0, (j) LoD3.1, (k) LoD3.2, and (l) LoD3.3.
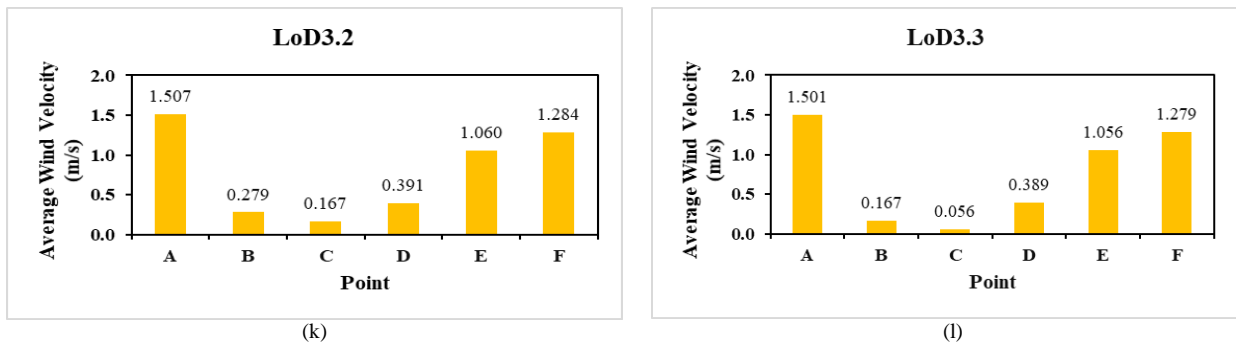
(k)

(l)

Figure 7.   Continued.

points B, E, and F have similar type of closed area that allows recirculation to happen, point C exists in a smaller area that enables the wind to accumulate in this small area, causing an even lower wind velocity.

The final trend can be obtained from LoD3.1, 3.2 and 3.3 graphs. The values at point A (1.571, 1.507, 1.501 m/s), B (0.28, 0.279, 0.167 m/s), C (0.168, 0.167, 0.056 m/s) and D (0.392, 0.391, 0.389 m/s) show the same trend as in the earlier graph, and for the same reasons that were discussed above. Nonetheless, points E (1.063, 1.06, 1.056 m/s) and F (1.287, 1.284, 1.279 m/s) labelled in these three models are in a hollow (allowing the wind to pass through) where E is at the wall and F is at the centre of the hollow shape. Point F experiences higher wind velocity than E because no obstacle blocks the wind passing through that area.

Besides, Table 1 below shows the percentage differences of wind velocity between the models involved. In the table, a column for LoD3.3 is shaded as it serves as the reference baseline for calculating the wind velocity differences, because this LoD3.3 model has the most detailed representation of the building design and can therefore be compared to all the less detailed models. Also, the percentage difference of the wind velocity is presented graphically in Figure 8.

Based on the first analysis, every single change in building shape can affect the wind velocity. So, the detailed building design will help produce a good representation of wind velocity at selected points of the shape. But, the analysis

of percentage differences is pursued to find the minimum requirements of building design detail, for used in wind flow calculations around the building. Building details can be obtained from the different LoDs used in this study. Hence, the minimum requirement can be acquired based an acceptable percentage difference from LoD3.3 wind velocity results. By assuming the percentage difference should be below 10%, all the results were assessed.

As for point A, LoD3.2 shows no difference in percentage value, which is 0% when rounded off to a whole number; meanwhile, LoD1.0 shows the biggest difference percentage (30%). Besides, it is different for Point B. LoD1.3 displays the least percentage difference of 11%, and the highest difference is for LoD1.0, which reaches up to 117%. But, LoD3.2 continues to have a small percentage difference from LoD3.3, around 1%, the same as for LoD3.1; and the largest difference was presented by LoD1.3 (63%) for point C. At the same point, no available value (#N/A) is recorded for LoD1.0 and 1.1. Proceeding to point D, LoD3.2 has roughly no difference in wind velocity, so it has the value 0%; however, 75% was produced from the calculation for LoD2.1 and 2.2 showing the largest differences from LoD3.3. As for points E and F, LoD3.2 still showed no difference or only 0%, but somehow, the highest percentage difference shows a different scenario. For point E, LoD1.2 has the largest difference (82%), and for point F, LoD1.1 followed LoD1.2 in showing the largest difference (85%). Based on points A, C, D, E and F, respectively, only LoD 3.1 and 3.2 fall within the
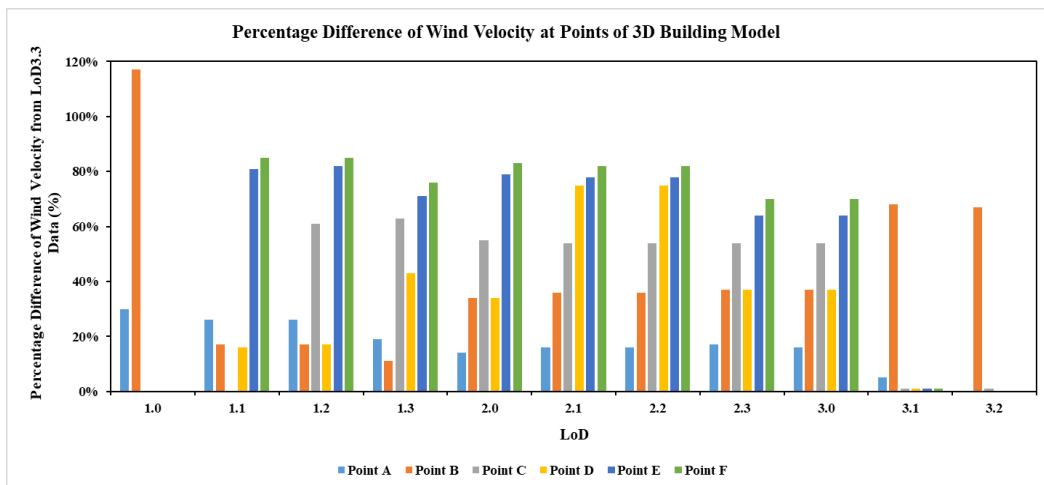

Figure 8.   Percentage difference of wind velocity at all points (A, B, C, D, E and F) of 3D building models from wind velocity for LoD3.3

requirement. Meanwhile, for point B, no model fulfils this requirement. So, to determine the suitable model for use in wind flow simulations, the model with the most points that fall within the acceptable percentage difference of wind velocity is selected. As from Table 1, LoD3.1 and 3.2 fit the defined criteria.

Additionally, Table 1 includes a column for documenting the Root Mean Square Error (RMSE) data used to validate the percentage differences in wind velocity. This column demonstrates that LoD3.1 and 3.2 have the lowest errors, at 0.054 and 0.046, respectively. This small inaccuracy shows that LoD3.1 and 3.2 models perform well (Raei, Ahmadi, Neyshaburi, Ghorbani, & Asadzadeh, 2021). Meanwhile, the remaining LoDs (LoD1.0–LoD3.0) recorded error values of 0.727, 0.591, 0.589, 0.520, 0.560, 0.570, 0.570, 0.476, and 0.476. Thus, with the exception of 3.3, both LoD3.1 and 3.2 are appropriate for CFD wind simulation. However, because the results are comparable to LoD3.3 and the design complexity is less than for the LoD3.2 model, LoD3.1 is designated as the minimum criterion for achieving good wind modelling results. Furthermore, Figure 9 presents the comparison between velocities from the chosen simulation domain of LoD3.1 and the reference domain of LoD3.3. The similarity between the outcomes from LoD3.1 and LoD3.3 simulations is assessed through the coefficient of determination, $R^2 = 0.9798$. This demonstrates a strong agreement between the two environments and backs the selection of LoD3.1.

4. Conclusions

This paper provides a study on the effects of different LoDs (LoD1.0, 1.1, 1.2, 1.3, 2.0, 2.1, 2.2, 2.3, 3.0, 3.1, 3.2 and 3.3) of building models on the wind flow from using CFD simulations. Each of these models has its own complexity level and they differ in geometry from one another. From the simulations of all the models, visualization of wind flow around the building can be obtained. At the same time, wind velocity analysis can be done based on the simulations. This analysis shows that wind velocity varies at the probed points along the simulation plane. Low wind

velocities prevail at a point located at or near an enclosed area, causing the wind to stall and lose its speed, such as point B, while a high velocity is at a point associated with open space that enables the wind to flow freely without any blockage or barrier, such as point F. To choose the suitable model to visualize wind flow, LoD3.3 wind velocity at every point was used as a reference to assess deviations of wind velocity for the different LoDs, because this model had the most detailed representation of the chosen building design and could be compared to any point available in the less detailed building models. Based on this analysis, LoD3.1 was selected as the lowest LoD that can fulfill the minimum requirement set, and gave an acceptable 0.054 RMSE and R^2 of 0.9682. Thus, with the provided study and analysis, a good representation of wind flow can be generated and this supports the aim of achieving sustainable development. For future development in this scope of the study, more parameters can be added to the CFD simulations; one example is pollutant data, which was not available in this current study.
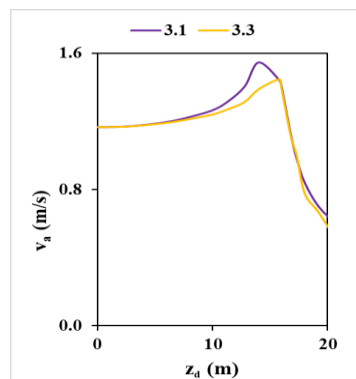
Figure 9. Comparison between LoD3.1 and LoD3.3 environments

Acknowledgements

Table 1. Percentage differences in wind velocity at points A, B, C, D, E and F from the baseline reference LoD3.3

LoD	Point A		Point B		Point C		Point D		Point E		Point F		RMSE
	$\bar{x}$ [1]	% [2]	$\bar{x}$	%	$\bar{x}$	%	$\bar{x}$	%	$\bar{x}$	%	$\bar{x}$	%	
1.0	1.951	30%	0.361	117%	#N/A	#N/A	#N/A	#N/A	#N/A	#N/A	#N/A	#N/A	0.727
1.1	1.891	26%	0.196	17%	#N/A	#N/A	0.326	16%	0.196	81%	0.196	85%	0.591
1.2	1.886	26%	0.195	17%	0.065	61%	0.455	17%	0.195	82%	0.195	85%	0.589
1.3	1.792	19%	0.185	11%	0.062	63%	0.556	43%	0.309	71%	0.309	76%	0.520
2.0	1.715	14%	0.224	34%	0.076	55%	0.522	34%	0.224	79%	0.224	83%	0.560
2.1	1.743	16%	0.227	36%	0.076	54%	0.682	75%	0.227	78%	0.227	82%	0.570
2.2	1.744	16%	0.227	36%	0.076	54%	0.682	75%	0.227	78%	0.227	82%	0.570
2.3	1.754	17%	0.229	37%	0.076	54%	0.534	37%	0.381	64%	0.381	70%	0.476
3.0	1.746	16%	0.223	37%	0.076	54%	0.531	37%	0.380	64%	0.3796	70%	0.476
3.1	1.571	5%	0.280	68%	0.168	1%	0.392	1%	1.063	1%	1.287	1%	0.054
3.2	1.507	0%	0.279	67%	0.167	1%	0.391	0%	1.060	0%	1.287	0%	0.046
3.3	1.501		0.167		0.166		0.389		1.056		1.279		

- Average wind velocity
- Percentage difference from wind velocity values of LoD 3.3 building model

References

Arroyo Ohori, K., Biljecki, F., Kumar, K., Ledoux, H., & Stoter, J. (2018). Modeling cities and landscapes in 3D with CityGML. *Building Information Modeling: Technology Foundations and Industry Practice*, 199–215. doi:10.1007/978-3-319-92862-3_11

Bettermann, S., Kandelhard, F., Moritz, H. U., & Pauer, W. (2019). Digital and lean development method for 3D-printed reactors based on CAD modeling and CFD simulation. *Chemical Engineering Research and Design*, *152*, 71–84. doi:10.1016/J.CHERD. 2019.09.024

Biao, L., Cunyan, J., Lu, W., Weihua, C., & Jing, L. (2019). A parametric study of the effect of building layout on wind flow over an urban area. *Building and Environment*, *160*, 106160. doi:10.1016/j.buildenv. 2019.106160

Biljecki, F, Ledoux, H., & Stoter, J. (2016). An improved LOD specification for 3D building models. *Computers, Environment, and Urban Systems*, *59*, 25–37. doi:10.1016/j.compenvurbsys.2016.04.005

Biljecki, Filip, Stoter, J., Ledoux, H., Zlatanova, S., & Çöltekin, A. (2015). Applications of 3D city models: State of the art review. *ISPRS International Journal of Geo-Information*, *4*(4), 2842–2889. doi:10.3390/ijgi4042842

Chatzimichailidis, A. E., Argyropoulos, C. D., Assael, M. J., & Kakosimos, K. E. (2019). Implicit definition of flow patterns in street canyons-recirculation zone-using exploratory quantitative and qualitative methods. *Atmosphere*, *10*(12), 794. doi:10.3390/ ATMOS10120794

Colucci, E., Ruvo, V. De, Lingua, A., Matrone, F., & Rizzo, G. (2020). HBIM-GIS integration: From IFC to CityGML standard for damaged cultural heritage in a multiscale 3D GIS. *Applied Sciences, 10*(4), 1356. doi:10.3390/APP10041356

Concentration, Heat and Momentum [CHAM]. (2020). *RhinoCFD (Version 2.1).* [Computer Software]. Retrieved from http://www.cham.co.uk/phoenics/ d_polis/d_enc/minires.htm

Deininger, M. E., Grün, M. von der, Piepereit, R., Schneider, S., Santhanavanich, T., Coors, V., & Voß, U. (2020). A continuous, semi-automated workflow: From 3D city models with geometric optimization and CFD simulations to visualization of wind in an urban environment. *ISPRS International Journal of Geo-Information*, *9*(11), 657. doi:10.3390/IJGI9110 657

Jang, Y. H., Park, S. I., Kwon, T. H., & Lee, S. H. (2021). CityGML urban model generation using national public datasets for flood damage simulations: A case study in Korea. *Journal of Environmental Management*, *297*, 113236. doi:10.1016/J.JENV MAN.2021.113236

Kutzner, T., Chaturvedi, K., & Kolbe, T. H. (2020). CityGML 3.0: New functions open up new applications. *PFG - Journal of Photogrammetry, Remote Sensing and Geoinformation Science*, *88*(1), 43–61. doi:10. 1007/s41064-020-00095-z

Lee, M., Park, G., Jang, H., & Kim, C. (2021). Development of building CFD model design process based on BIM. *Applied Sciences, 11*(3), 1252. doi:10. 3390/APP11031252

Lee, M., Park, G., Park, C., & Kim, C. (2020). Improvement of grid independence test for computational fluid dynamics model of building based on grid resolution. *Advances in Civil Engineering*, *2020*. doi:10.1155/2020/8827936

Liu, J., Niu, J., Mak, C. M., & Xia, Q. (2017). Detached eddy simulation of pedestrian-level wind and gust around an elevated building. *Building and Environment*, *125*, 168–179. doi:10.1016/j.buildenv.2017.08.031

Lu, L., Becker, T., & Löwner, M.-O. (2017). 3D complete traffic noise analysis based on CityGML. *Advances in 3D Geoinformation*, *0*(9783319256894), 265–283. doi:10.1007/978-3-319-25691-7_15

Piepereit, R., Deininger, M., Kada, M., Pries, M., & Voß, U. (2018). A sweep-plane algorithm for the simplification of 3D building models in the application scenario of wind simulations. *International Archives of the Photogrammetry, Remote Sensing and Spatial Information Sciences - ISPRS Archives*, *42*(4/W10), 151–156. doi:10. 5194/isprs-archives-XLII-4-W10-151-2018

Raei, B., Ahmadi, A., Neyshaburi, M. R., Ghorbani, M. A., & Asadzadeh, F. (2021). Comparative evaluation of the whale optimization algorithm and backpropagation for training neural networks to model soil wind erodibility. *Arabian Journal of Geosciences*, *14*(1), 1–19. doi:10.1007/S12517-020-06328-0/FIGURES/12

Tang, L., Li, L., Ying, S., & Lei, Y. (2018). A full level-of-detail specification for 3D building models combining indoor and outdoor scenes. *ISPRS International Journal of Geo-Information*, *7*(11), 419. doi:10.3390/IJGI7110419

Tey, W. Y., Asako, Y., Sidik, N. A. C., & Goh, R. Z. (2017). Governing equations in computational fluid dynamics: Derivations and a recent review. *Progress in Energy and Environment*, *1*, 1–19. Retrieved from https://www.akademiabaru.com/ submit/index.php/progee/article/view/1026

Triscone, G., Abdennadher, N., Balisteri, C., Donze, O., Greco, D., Haas, P., … Despot, F. (2016). Computational fluid dynamics as a tool to predict the air pollution dispersion in a neighborhood – A research project to improve the quality of life in cities. *International Journal of Sustainable Development and Planning*, *11*(4), 546–557. doi:10.2495/SDP-V11-N4-546-557

van Druenen, T., van Hooff, T., Montazeri, H., & Blocken, B. (2019). CFD evaluation of building geometry modifications to reduce pedestrian-level wind speed. *Building and Environment*, *163*, 106293. doi:10. 1016/j.buildenv.2019.106293

Zawawi, M. H., Saleha, A., Salwa, A., Hassan, N. H., Zahari, N. M., Ramli, M. Z., & Muda, Z. C. (2018). A review: Fundamentals of computational fluid dynamics (CFD). *AIP Conference Proceedings*, *2030*(1), 020252. doi:10.1063/1.5066893